

Self-sustained gigahertz electronic oscillations in ultrahigh- Q photonic microresonators

Mohammad Soltani,^{*} Siva Yegnanarayanan,[†] Qing Li, Ali A. Eftekhari, and Ali Adibi[‡]

School of Electrical and Computer Engineering, Georgia Institute of Technology, Atlanta, Georgia 30332, USA

(Received 15 July 2011; published 17 May 2012)

We report on theoretical and experimental observations of self-sustained fast [gigahertz (GHz)] electronic oscillations resulting from coupled electron-photon dynamics in ultrahigh- Q Si microdisk resonators with cw pumping. Our theoretical analysis identifies conditions for generating steady-state GHz oscillations while suppressing thermal oscillations [megahertz (MHz)] with submilliwatt input laser power. Such fast oscillations are tunable via changing the free-carrier (FC) lifetime of the resonator. Integrating a p - i - n diode with these high- Q resonators for controlling the FC lifetime promises the realization of an integrated voltage-controlled oscillator (VCO) in a silicon photonics chip.

DOI: [10.1103/PhysRevA.85.053819](https://doi.org/10.1103/PhysRevA.85.053819)

PACS number(s): 42.60.Da, 42.82.-m, 78.67.-n, 05.45.-a

I. INTRODUCTION

Whispering gallery mode (WGM) resonators have been promising in light-matter interaction studies and realization of on-chip optical devices [1–3]. The structural simplicity, high Q , and low mode volume (V_m) of a WGM resonator in addition to its efficient coupling to a waveguide on the same substrate have enabled these studies at milliwatt (mW) and sub-mW optical powers. In recent studies, generation of self-sustained oscillations in these resonators has been pursued. Examples include generation of ultralow phase noise microwave oscillations using parametric nonlinear optics in a WGM resonator [4], radiation pressure induced coupling of optical and mechanical modes in a WGM resonator for generating optomechanical oscillations [5–7], and generation of microwave oscillations excited by radiation pressure via the stimulated Brillouin scattering [8]. In silicon microdisks, simultaneous two-photon absorption (TPA) (due to the strong buildup of light intensity in the resonator) and self-heating (cooling) of the resonator have resulted in thermal oscillations in the megahertz (MHz) range [9]. In this article, we report the observation of optically excited oscillations in an on-chip Si microdisk resonator at microwave rates (~ 1 GHz). These oscillations are the outcome of the tight coupling of photon and electron dynamics in Si high- Q resonators. We show the conditions for the generation of pure and self-sustained fast oscillations (in the GHz regime) in the absence of slow (thermal) oscillations. The frequency of these oscillations can be tuned with resonator parameters such as resonator free-carrier (FC) lifetime.

II. THEORETICAL ANALYSIS OF SELF-SUSTAINED OSCILLATIONS

Before attempting to understand the nature of these fast oscillations, we qualitatively summarize the general physical

processes in a Si traveling wave resonator (TWR) critically coupled to a waveguide [as schematically shown in Fig. 1(a)] at high powers: (1) the loss of photons due to TPA; (2) the generation of FCs as a consequence of TPA and further photon loss due to excess Ohmic loss; (3) reduction of Q (broadening of linewidth) as the outcome of (1) and (2); (4) deviation from the critical coupling condition due to the Q reduction, which reduces the power buildup in the resonator; (5) resonance shift caused by FCs (blue shift) and by self-heating and thermo-optic effect (red shift). The final outcome of all the above effects is broadening and asymmetry in the spectral response of the resonator (which is originally Lorentzian). At some portions of this distorted spectrum, the resonator is temporally unstable, which results in self-oscillation.

A quantitative spectral and temporal dynamic analysis of a TWR coupled to a waveguide can be performed using coupled-mode theory [10]. In this analysis, an amplitude a (S_{in}) and phase ϕ_a (ϕ_{in}) are designated to the resonator mode (input waveguide mode). The resonator (waveguide) mode is normalized such that the squared magnitude of a (S_{in}) represents the resonator energy U (waveguide input power P_{in}). By modifying the coupled-mode equations from the amplitude to the energy form we have [11]

$$\begin{aligned} dU/dt &= [-\omega_0/Q_L]U + 2\kappa\sqrt{P_{in}U}\cos(\phi_a - \phi_{in}), \\ d\phi_a/dt &= [\Delta\omega_0(t) - \delta\omega_L] - \kappa\sqrt{P_{in}/U}\sin(\phi_a - \phi_{in}), \\ P_{out} &= |S_{in}e^{i\phi_{in}} - \kappa^*a e^{i\phi_a}|^2, \\ \Delta\omega_0(t)/\omega_0 &= -[\Delta n(t)]_\theta + \Delta n(t)|_{FC}/n_{Si}, \end{aligned} \quad (1)$$

where ω_0 is the resonator cold resonance frequency; κ is the waveguide-resonator coupling constant, which is related to the waveguide-resonator coupling Q (Q_e) as $|\kappa|^2 = \omega_0/Q_e$ (without lack of generality we assume that κ is real); P_{out} is the waveguide output power; $\delta\omega_L$ is the detuning of the laser frequency from the resonator cold frequency (i.e., $\delta\omega_L = \omega_{Laser} - \omega_0$); $\Delta\omega_0$ is the resonance shift of the resonator mainly due to refractive index change induced by thermo-optic ($\Delta n|_\theta = A_{th}\theta$, $A_{th} = 1.84 \times 10^{-4} \text{ K}^{-1}$, θ is temperature) and FC dispersion ($\Delta n|_{FC}$) [9]. The refractive index change due to the Kerr effect is very weak and can be neglected. In Eq. (1), Q_L is the loaded Q of the resonator, which is composed of three parts: (1) Q_0 , (2) Q_e , and (3) the nonlinear contribution which includes Q_{TPA} (due to TPA loss) and Q_{FC} (due to TPA-induced

^{*}Present address: Laboratory of Atomic and Solid State Physics, Physics Department, Cornell University, Ithaca, New York 14850, USA.

[†]Present address: MIT Lincoln Laboratory, 244 Wood St., Lexington, Massachusetts 02420, USA.

[‡]Corresponding author: adibi@ece.gatech.edu

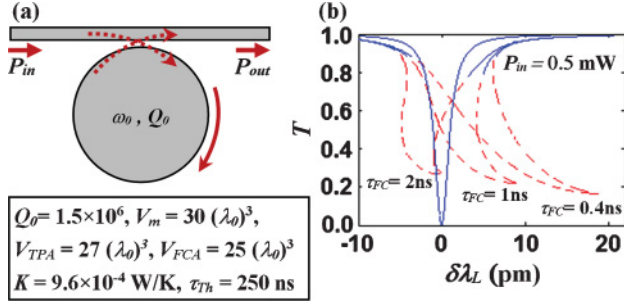


FIG. 1. (Color) (a) Schematic of a waveguide-TWR coupling. (b) Theoretical results for the variation of the transmission coefficient (P_{out}/P_{in}) versus laser wavelength detuned from the cold resonance of the TWR at different FC lifetimes. The symmetric Lorentzian in this figure is the linear low input power spectrum of the device. The resonator parameters are shown in the box.

FC loss). Therefore, we have

$$Q_L^{-1} = Q_0^{-1} + Q_e^{-1} + Q_{TPA}^{-1} + Q_{FC}^{-1}. \quad (2)$$

Using the expression for TPA power loss, $P_{TPA} = c^2 \beta U / (2\hbar \omega_0 n_g^2 V_{TPA})$, in which c is the light velocity, β is the TPA coefficient, n_g is the group index of the TWR mode, and V_{TPA} is the effective TPA mode volume [9]) and FC loss [9], Q_L can be expressed in terms of the resonator energy and FC density. The equations governing the dynamics of the FC density (N) and the temperature rise (θ) in the resonator are

$$\begin{aligned} dN/dt &= -N/\tau_{FC} + G_{FCA}U^2, \\ d\theta/dt &= -\theta/\tau_{Th} + P_{abs}/(K\tau_{Th}). \end{aligned} \quad (3)$$

In these equations, τ_{FC} is the FC lifetime; τ_{Th} and K are the thermal lifetime and thermal conductance of the resonator, respectively; and $G_{FCA} = c^2 \beta / (2\hbar \omega_0 n_g^2 V_{FCA}^2)$ in which V_{FCA} is the effective mode volume in which FCs are concentrated [9]. P_{abs} is the power absorbed by the resonator, which is expressed as

$$P_{abs}(t) = \omega_0 Q_a^{-1} U = \omega_0 [\eta Q_0^{-1} + Q_{TPA}^{-1}(t) + Q_{FC}^{-1}(t)] U, \quad (4)$$

where Q_a is the contribution of the resonator Q from the total absorption. η is the fraction of Q_0 contributed from the linear absorption. In Si ultrahigh- Q TWR studied here Q_0 is predominantly due to surface-state absorption [12]. Hence, with a good approximation we have $\eta \approx 1$. The first two equations in system (1) and the two equations in system (3) form the four state equations of the resonator. These equations can be analyzed in both steady-state ($d/dt = 0$) and temporal regimes. For the analysis we choose a microdisk with a radius of 20 μm and a thickness of 230 nm in a silicon-on-insulator (SOI) substrate with a buried oxide (BOX) thickness of 1 μm . A 50-nm Si slab is at the interface between the Si layer and the BOX layer to improve thermal heat sink [13] as well as improving the waveguide-resonator coupling [14]. Figure 1(b) shows a theoretical steady-state transmission spectrum of the resonator versus the input laser wavelength detuned from the cold resonance wavelength (i.e., $\delta\lambda_L = \lambda_L - \lambda_0$) in the linear and nonlinear (high input power, P_{in}) regimes for three different FC lifetimes as indicated in the figure. From Fig. 1(b)

asymmetry and broadening in the spectrum and the way they change with varying FC lifetime are clearly observed. The dashed portions of each plot in Fig. 1(b) show the regions in which the resonator is temporally unstable. These instability regions in Fig. 1(b) are determined through the resonator stability analysis by perturbing the state variables of the resonator [U, ϕ_a, N, θ] from their steady-state values. The perturbed values are designated as [$\delta U, \delta\phi_a, \delta N, \delta\theta$]. Putting these in the aforementioned equations and using the first-order Taylor expansion, a new 4×4 equation can be formed as

$$[\delta\dot{U}, \delta\dot{\phi}, \delta\dot{N}, \delta\dot{\theta}]' = [D]_{4 \times 4} [\delta U, \delta\phi, \delta N, \delta\theta]', \quad (5)$$

where D is a 4×4 Jacobian matrix. If the real parts of all four eigenvalues of D are negative, then the resonator is stable at the corresponding wavelength. Otherwise, oscillations can be observed. Recent experimental results have shown oscillations with frequencies in the range of a sub-MHz to a few MHz. We show here that even faster oscillations in the GHz range are possible. In fact the appearance and lack of damping of the fast oscillations require a resonator with a high thermal conductance or a weak thermo-optic effect. In the former experiments, the resonators were undercut which resulted in a very poor thermal conductance for the resonator [9]. For our resonator, from a separate analysis by solving the heat equation with the resonator mode loss as the heat source, we found the self-heating thermal conductance of the resonator to be 9.6×10^{-4} W/K, which was much larger than those of undercut resonators with similar dimensions. Figure 2 shows the simulation results for the temporal response of a microdisk resonator. Figure 2(a) shows simultaneous slow and fast oscillations in the output power. As seen from Fig. 2(a), the fast oscillations cover a portion of a duty cycle of slow oscillations. In our studies we observed that by increasing (decreasing) the input power, the number of the cycles of the fast oscillations

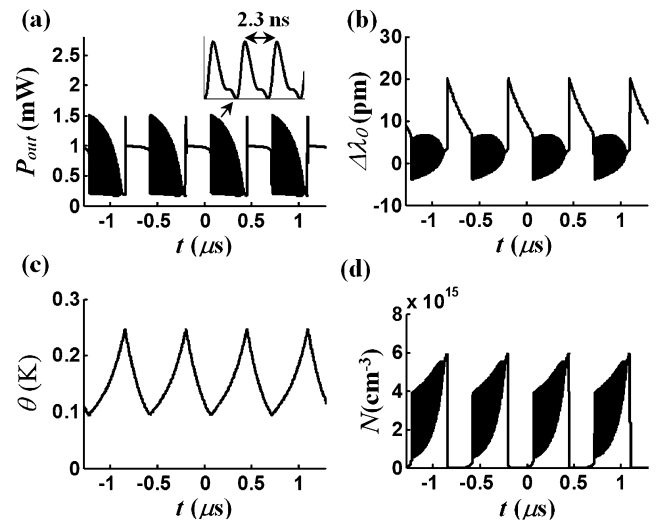


FIG. 2. Theoretical demonstration of simultaneous slow and fast oscillations in the response of the waveguide-TWR structure in Fig. 1(a): (a) Output power of the waveguide, (b) resonance wavelength change, (c) temperature, and (d) FC density as functions of time. For this analysis, $P_{in} = 0.5$ mW, $\delta\omega = 3\omega_0/Q_0$, $\tau_{FC} = 0.4$ ns, and the rest of the parameters are given in the box in Fig. 1.

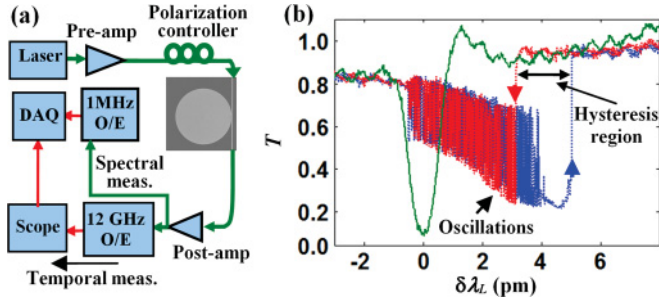


FIG. 3. (Color) (a) Experimental setup used for monitoring the time-domain and spectral-domain response of the resonator. The scanning electron microscopy (SEM) image of the measured microdisk is shown in the setup. (b) Measured resonance transmission ($T = P_{\text{out}}/P_{\text{in}}$) spectrum at low powers (the solid green curve) and at high powers ($P_{\text{in}} \approx 200 \mu\text{W}$) when the input laser wavelength is swept from left to right (the dotted blue curve) and from right to left (the dotted red curves). $\delta\lambda_L$ is the laser wavelength detuning from the cavity resonance. The resonance wavelength is near 1532 nm.

was increased (decreased). Also Figs. 2(b)–2(d) show the temporal variation of resonance wavelength, temperature, and FC density, respectively.

III. EXPERIMENTAL RESULTS

For the experimental analysis, the fabricated Si microdisk had a radius of $20 \mu\text{m}$ and a thickness of 230 nm seated on a $1\text{-}\mu\text{m}$ SiO_2 BOX layer in a SOI platform. The measured slab thickness (as mentioned before) was 40 nm. The details of the fabrication can be found in Ref. [14]. Figure 3(a) shows the experimental setup. A tunable laser followed by an amplifier is used as the light source. A fiber polarization controller tunes the polarization to transverse electric (TE, i.e. the electric field is in-plane with the microdisk) before launching it into the waveguide-resonator device. The output optical signal after being postamplified is separated into two paths: (1) one to measure the spectral line shape of the resonator when changing the input laser wavelength, and (2) the other to measure the temporal oscillatory behavior of the resonator for a fixed laser wavelength. In path 2, the optical signal is sent to a high-speed oscilloscope through a high-speed optoelectronic (O/E) converter. In this experiment, we had a series of resonators on chip, and the measured Q for them was in the range of $(1\text{--}3) \times 10^6$. Based on this, all the theoretical simulations were performed for a resonator with $Q=1.5 \times 10^6$. Figure 3(b) shows the spectral line shape of the resonator at low powers (green curve) and high powers when scanning the laser wavelength from low to high (blue curve) and from high to low (red curve) wavelength. For this resonator, the intrinsic Q is $\sim 2 \times 10^6$.

From Fig. 3(b), instability in the response of the resonator is observed. Also a hysteresis region can be found when sweeping the laser wavelength from low to high and then from high to low. Figure 4(a) shows the experimental verification of simultaneous slow and fast oscillation for the microdisk shown in Fig. 3(a). The laser wavelength is fixed and red tuned with respect to the cold resonance of the resonator

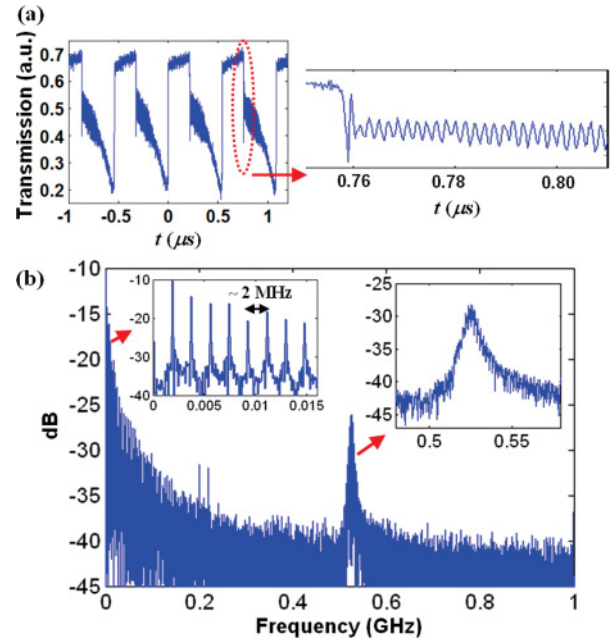


FIG. 4. (Color online) Experimental results for temporal oscillations of the microdisk resonator shown in Fig. 3(a). (a) Observation of simultaneous steady-state slow (MHz) and fast (GHz) oscillations. A zoomed view of the fast oscillation is shown on the right. (b) Spectrum of the oscillations. The left inset shows the spectral components of the slow oscillations, and the right inset shows the spectrum of the fast oscillations.

within a few picometers. Figure 4(b) shows the frequency spectrum of the oscillations in which both slow and fast portions of the oscillations are clear. The spectrum of the fast oscillations is broad which is mainly due to the presence of sharp steplike transitions in slow oscillations. Hence, an interesting case is to suppress the slow oscillations and preserve the fast oscillations to significantly reduce the linewidth of the fast oscillations. This is the situation which was not observed in our resonator under the experiment. This is mainly because of short FC lifetime ($\sim 400\text{--}500$ ps, after fitting experimental data to theory) of our resonator. This will be further clarified in the rest of the paper by finding approximate conditions for the resonator parameters under which the resonator will show purely fast oscillations.

IV. CONDITIONS FOR OBTAINING PURE FAST OSCILLATIONS

Knowing that slow and fast oscillations have two very different time scales, we can analyze fast oscillations by assuming that thermal behavior is so slow that we can assume the temperature is constant (equal to its steady-state value). Therefore, the state equations reduce to three in the following form: $[\delta U \delta \phi \delta N] = [M_N]_{3 \times 3} [\delta U \delta \phi \delta N]$. By finding the eigenvalues of M_N and assuring that at least one of them has a positive real part, the following condition for having fast

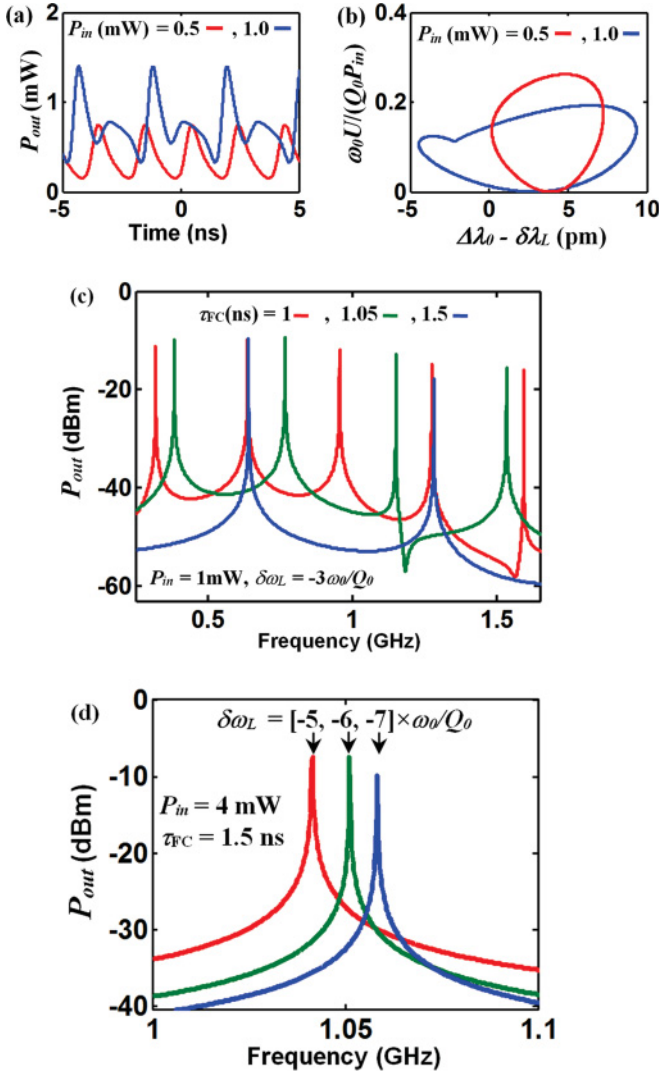


FIG. 5. (Color) Generation of pure fast oscillations. (a) Onset of fast oscillations of the waveguide-TWR at two input power levels of 0.5 mW (red) and 1 mW (blue), and; (b) the contour plots of resonator normalized energy versus resonance wavelength change ($\Delta\lambda_0$) with respect to laser detuning ($\delta\lambda_L$); In (a) and (b), $\delta\omega = 3\omega_0/Q_0$ and $\tau_{FC} = 1$ ns. (c) Spectrum of the output power for different FC lifetimes as indicated; In (c), $P_{in} = 1$ mW and $\delta\omega = 3\omega_0/Q_0$. (d) Spectrum of the first harmonic of the oscillations at different laser detuning levels. In (d), $P_{in} = 4$ mW and $\tau_{FC} = 1.5$ ns. The box in Fig. 1 contains the rest of the resonator parameters for the above simulations.

oscillations is obtained [11]:

$$4G_{TPA}\tau_{FC}^2U^2\left[\frac{\Delta\omega_0 - \delta\omega_L}{n_{Si}}\frac{\partial\Delta n|_{FC}}{\partial N} - \frac{1}{2}\left(\frac{\omega_0}{2Q_L} - \frac{1}{\tau_{FC}}\right)\right] + \frac{\partial}{\partial N}\left(\frac{1}{Q_L}\right) + \frac{\partial}{\partial U}\left(\frac{U}{Q_L}\right) < 0. \quad (6)$$

Similarly, we can find the condition in which slow oscillations are absent. In this case, the FC dynamics is so fast compared to thermal dynamics that we can assume it responds instantaneously [15]. Therefore, the state equations reduce to three in the following form: $[\delta\dot{U}\delta\dot{\phi}\delta\dot{\theta}] = [M_\theta]_{3\times 3}[\delta U\delta\phi\delta\theta]$.

By finding the eigenvalues of M_θ and forcing their real parts to be negative, the following condition for stability can be obtained [11]:

$$\left[2\frac{A_{th}}{K\tau_{Th}}\frac{\omega_0U}{n_{Si}}(\Delta\omega_0 - \delta\omega_L) + 1\right]\frac{\partial}{\partial U}\left(\frac{U}{Q_a}\right) + \frac{1}{Q_e} > 0. \quad (7)$$

Equations (6) and (7) provide us approximate conditions and the way resonator parameters should be in order to only have the fast oscillations. From Eq. (7), we notice that all the resonator thermal effects are explicitly compacted in the term $A_{th}/(K\tau_{Th})$. In addition the thermal and FC effects are implicitly present as well in Eq. (7) in $\Delta\omega_0$. If a resonator has a poor thermal property (i.e., large A_{th} , small K , and large τ_{Th}), the resonance is strongly red shifted (i.e., $\Delta\omega_0$ is strongly negative), and the term $A_{th}/(K\tau_{Th})$ is also very large, and therefore the term in the bracket in Eq. (7) can become negative which makes it hard to satisfy Eq. (7) anymore.

Figure 5(a) shows the simulation results of the dynamical Eqs. (1) and (3) with the resonator parameters that suppress the slow oscillations and only produce fast oscillations. The shown oscillations in Fig. 5(a) are for two input powers of 0.5 and 1 mW and, with the given resonator parameters, are achievable in practice. All the resonator parameters in Figs. 2 and 5(a) (red curve) are similar except the FC lifetime which has increased to 1 ns. This increase in the FC lifetime satisfies Eqs. (6) and (7) which have τ_{FC} explicitly or implicitly through $\Delta\omega_0$, U , Q_a , Q_L , and $\Delta n|_{FC}$. The oscillations in Fig. 5(a) are not purely sinusoidal, which means higher harmonics are present. Figure 5(b) shows the contour plot of the resonator energy versus the resonance wavelength for the two power levels. As seen from this figure, the contours are closed loop indicating self-sustained oscillations. All the remaining resonator parameters are shown in the box in Fig. 1, and they are practically realistic numbers. Therefore, we note that with reasonable improvement of the fabrication, GHz oscillations are within reach. An interesting observation is the spectrum of the oscillations shown in Fig. 5(c), where combine higher harmonics of the fast oscillations are present (the spectra are simulated for different FC lifetimes). The presence of higher harmonics is because of the nonlinearity of the governing equations. As seen from Fig. 5(c), by tuning the FC lifetime, the oscillation frequency can be modified. In practice, the FC lifetime tuning can be done by integrating a p - i - n diode with the resonator and operating it in the reverse voltage bias [16]. This promises the realization of an integrated VCO in a silicon photonic platform. Figure 5(d) shows the spectrum of the first harmonic of the oscillations at different laser detuning levels for the input power and FC lifetime specified in the figure. From this figure we can say that by tuning the laser within a few resonator linewidths (ω_0/Q_0), the GHz oscillations can be still achieved.

V. CONCLUSION

In conclusion, we have shown that self-sustained GHz electronic oscillation can be generated within a Si photonic microresonator using a low-power continuous laser. Our experimental data show the simultaneous appearance of slow and fast oscillation in the resonator. In addition, our theoretical analysis finds the resonator parameters and conditions under

which the resonator can generate pure fast (GHz) oscillations. The period of these pure fast oscillations can be controlled by changing the resonator FC lifetime. In principle, by integrating a reversely biased $p-i-n$ diode with the resonator which functions as a FC lifetime controller, an integrated VCO can be achieved. Such an optoelectronic oscillator scheme promises the realization of high-frequency tunable clocks in a microphotonic platform for RF and microwave signaling processing applications. Further work on this oscillator is

its integration with a $p-i-n$ diode, studying the phase noise of this oscillator, and extending the oscillation frequency to multi-GHz frequencies.

ACKNOWLEDGMENTS

This work was supported in part by the Air Force Office of Scientific Research under Contract No. FA9550-06-01-2003 (G. Pomrenke).

-
- [1] A. B. Matsko and V. S. Ilchenko, *IEEE J. Sel. Top. Quantum Electron.* **12**, 3 (2006).
 - [2] A. B. Matsko and V. S. Ilchenko, *IEEE J. Sel. Top. Quantum Electron.* **12**, 15 (2006).
 - [3] K. Vahala, *Nature* **424**, 839 (2003).
 - [4] V. S. Ilchenko, J. Byrd, A. A. Savchenkov, A. B. Matsko, D. Seidel, and L. Maleki, in *Frequency Control Symposium, 2008 IEEE International, Honolulu, HI* (IEEE, New York, 2008), pp. 305–308.
 - [5] T. J. Kippenberg, H. Rokhsari, T. Carmon, A. Scherer, and K. J. Vahala, *Phys. Rev. Lett.* **95**, 033901 (2005).
 - [6] A. Schliesser, P. Del’Haye, N. Nooshi, K. J. Vahala, and T. J. Kippenberg, *Phys. Rev. Lett.* **97**, 243905 (2006).
 - [7] Q. Lin, J. Rosenberg, X. Jiang, K. J. Vahala, and O. Painter, *Phys. Rev. Lett.* **103**, 103601 (2009).
 - [8] M. Tomes and Tal Carmon, *Phys. Rev. Lett.* **102**, 113601 (2009).
 - [9] T. Johnson, M. Borselli, and O. Painter, *Opt. Express* **14**, 817 (2006).
 - [10] C. Manolatou, M. J. Khan, S. Fan, P. R. Villeneuve, H. A. Haus, and J. D. Joannopoulos, *J. Lightwave Technol.* **35**, 1322 (1999).
 - [11] See Supplemental Material at <http://link.aps.org/supplemental/10.1103/PhysRevA.85.053819> for the details of derivation.
 - [12] M. Borselli, T. Johnson, and O. Painter, *Opt. Express* **13**, 1515 (2005).
 - [13] M. Soltani, S. Yegnanarayanan, Q. Li, and A. Adibi, *Opt. Express* **15**, 17305 (2007).
 - [14] M. Soltani, S. Yegnanarayanan, A. Adibi, *Opt. Express* **15**, 4694 (2007).
 - [15] In general we can assume that photon dynamics is also instantaneous; but this assumption makes finding a well-formed condition difficult.
 - [16] A. C. Turner-Foster, M. Foster, J. S. Levy, C. B. Poitras, R. Salem, A. L. Gaeta, and M. Lipson, *Opt. Express* **18**, 3582 (2010).